Synthesized Blue Fluorescent Protein Analogue with Tunable Colors from Excited-State Intramolecular Proton Transfer through an N-H···N Hydrogen Bond

ARTICLE *in* JOURNAL OF PHYSICAL CHEMISTRY LETTERS · DECEMBER 2013

Impact Factor: 7.46 · DOI: 10.1021/jz402280w

THE JOURNAL OF PHYSICAL CHEMISTRY Letters

Letter

pubs.acs.org/JPCL

Synthesized Blue Fluorescent Protein Analogue with Tunable Colors from Excited-State Intramolecular Proton Transfer through an N−H···N Hydrogen Bond

Xinxiu Fang,[†] Yan Wang,[§] Dan Wang,[‡] Guiyan Zhao,[†] Wenwen Zhang,[†] Aimin Ren,[‡] Haiyu Wang,[§] Jingwei Xu,*[,†] Bing-Rong Gao,*[,§] and Wei Yang*[,†]

[†]The State Key Laboratory of Electroanalytic Chemistry, Changchun Institute of Applied Chemistry, Chinese Academy of Sciences, Changchun 130022, China

[§]State Key Laboratory on Integrated Optoelectronics, College of Electronic Science and Engineering and [‡]State Key Laboratory of Theoretical and Computational Chemistry, Institute of Theoretical Chemistry, Jilin University, Changchun 130012, China

Supporting Information

ABSTRACT: A synthesized blue fluorescent protein (BFP) chromophore analogue 2-BFP ((4*Z*)-4-[(1H-imidazol-2-yl)methylene]-1-methyl-2-phenyl-1H-imidazol-5(4H)-one) displays dual fluorescent emission that arises from the same *Z*-isomer. The larger Stokes shift emission is a result of excited-state intramolecular proton transfer (ESIPT) mediated by an N−H···N type of hydrogen bond. Compared to other green fluorescent protein (GFP) analogues with ESIPT such as *o*-HBDI, 2-BFP possesses greatly enhanced quantum yields and much slower proton-transfer rates. In addition, fluorescence up-conversion experiments revealed two rising components of lifetime for the tautomer formation of 2-BFP. The results imply that the relaxation of the N* state in 2-BFP triggers the proton transfer of the molecule. The weaker photoacidity of N−H is proposed to be crucial for these photophysical and photochemical properties. Finally, the ESIPT process in 2-BFP is inhibited in protic solvents (MeOH) or by the formation of metal−chelate complexes, providing insights for further developments and applications of ESIPT molecules.

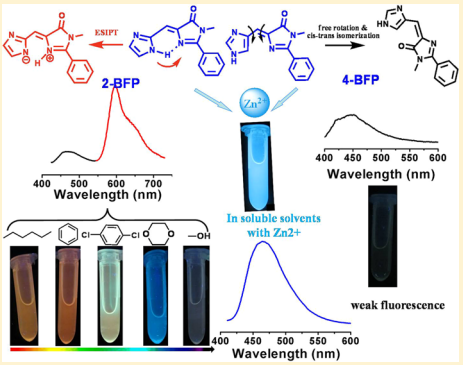

SECTION: Spectroscopy, Photochemistry, and Excited States

Because the green fluorescent protein (GFP) shows its unique and outstanding performance in biolabeling and bioimaging,[1−4] a series of derivatives including blue fluorescent protein (BFP) have been developed.[5,6] In recent years, besides the development of the FP color palette by protein technology,[7] efforts have been made to reveal the fundamental principles of their synthetic chromophore analogues,[8,9] which is essential for the further tailored design of novel fluorescent proteins as well as for the direct applications of these chromophore molecules. For example, the modification of *p*-HBDI analogues at the C(1) position (Figure 1) leads to a better understanding of the relationship between the chromophore structures and the luminescence mechanisms of the proteins.[10] Moreover, different proton-transfer processes have been revealed in GFP chromophore analogues *p*-, *m*-, and *o*-HBDI.[11−15]

For *p*-HBDI, excited-state proton transfer (ESPT) occurs via the proton relay of the active-site residues in the protein and the surrounding water network to remote residue but has not been observed in solvents for the free moiety.[11,12] The *m*-HBDI undergoes ultrafast intermolecular ESPT in aqueous solutions.[12,13] In stark contrast, an ESIPT arises via a seven-membered ring hydrogen-bonding system in *o*-HBDI, which shifts the emission to a unique longer wavelength (∼600 nm).[14,15] Unfortunately, the quantum yield of this emission is too low for its further applications. Recently, two highly fluorescent GFP-type chromophores possessing the intermolecular ESPT have also been published.[16]

Because of its spectral sensitivity to an environmental medium and the appearance of a large Stokes-shifted fluorescence, ESIPT reaction is considered as one of the most fundamental processes in chemistry and biology fields and has attracted keen interests.[17−22] ESIPT takes place in aromatic molecules that contain a proton donor (−OH or −NH) and a proton acceptor (O═C< or N≤) or a π-system.[19] The organic OH mediates the ESIPT most frequently due to the formation of a strong hydrogen bond (HB). Conversely, the relative weakness of the N−H···N HB generates an appreciably larger barrier for the proton transfer, which makes the ESIPT in this type of molecules rare.[18,23,24] Moreover, though the N−H···N type of intramolecular HB has been confirmed in BFP analogues (here, the GFP type of chromophores with two

Received: October 21, 2013
Accepted: December 9, 2013
Published: December 9, 2013

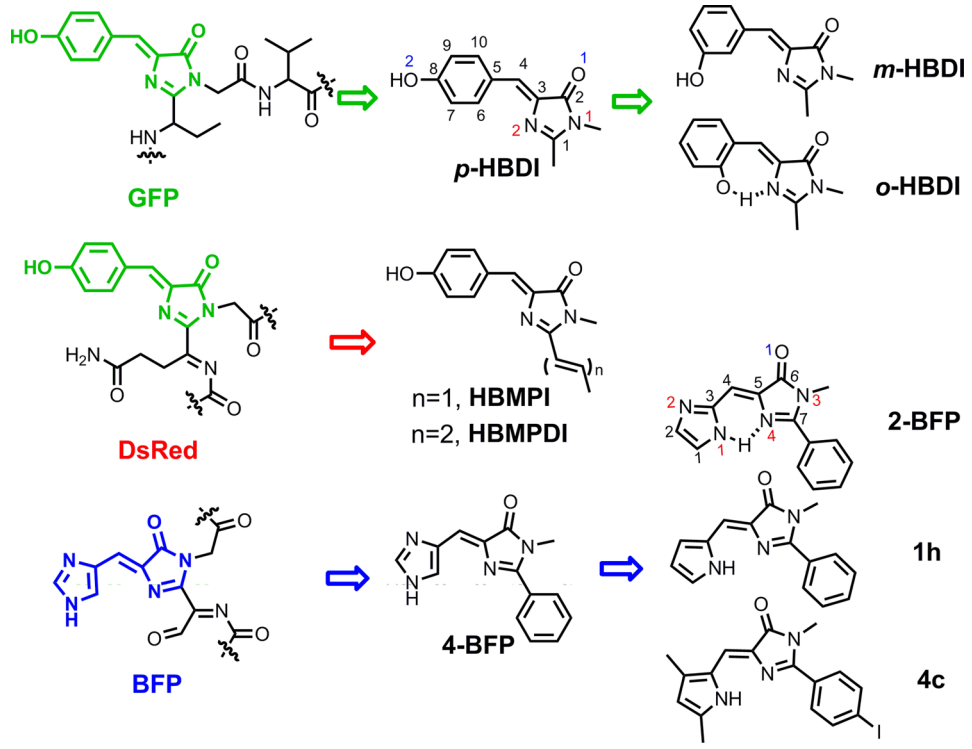

Figure 1. Structure of the GFP, DsRed, BFP, and respective derivative chromophores, *p*-HBDI, *m*-HBDI, *o*-HBDI, HBMPI, HBMPDI, 4-BFP, 2-BFP, 1h, and 4c.

imidazole rings or with one imidazole and one five-membered N-containing rings are denoted as BFP analogues; see Figure 1), no ESIPT process has been reported to date.[25,26] This arouses enigmas on BFP and its analogues. For example, does the BFP undergo proton transfer as GFP or not? If proton transfer occurs, is there any fundamental difference between the GFP and BFP analogues? The answers to these questions are crucial for designing applicable analogues of the fluorescent proteins or chromophores with proton transfers. In this study, it is found that a Zn^{2+}-dependent BFP analogue IMMPI ((4*Z*)-4-[(1H-imidazol-2-yl)methylene]-1-methyl-2-phenyl-1H-imidazol-5(4H)-one), hereafter, denoted as 2-BFP),[27] displays strong dual-emission fluorescence in aprotic solvents. Detailed analysis reveals that the longer-wavelength emission resulted from an ESIPT process with a quite different mechanism from that of GFP analogues.

The absorption spectra show only one maximum at ∼395 nm for 2-BFP with minor differences in various solvents (Figure 3). The high molar extinction coefficient (1.6−2.4 × 10^4 M^{-1} cm^{-1}) suggests a characteristic $\pi \rightarrow \pi^*$ transition. Differently, dual fluorescence is detected at around 470 (N band) and 595 nm (T band) with a shoulder at 635 nm in aprotic nonpolar solvents. In a comparative study, the analogue 4-BFP or 2-BFP/Zn^{2+} complex exhibits only N band emission. This validates that the blue emission is directly from a locally excited state (LE state: N*) while the emission with anomalously large Stokes shifts is unequivocally ascribed to the proton-transfer tautomer (T) emission. In addition, the fluorescence excitation spectra monitored at N and T bands are almost identical to the absorption spectrum, indicating that the entire emission results from a common Franck−Condon excited state.[28]

Structure analyses imply an ESIPT mediated by the N−H···N type of intramolecular HB in the *Z*-isomer of 2-BFP. At room temperature, only the *Z*-isomer was observed for 2-BFP in ^1H and ^{13}C NMR spectra. For example, the proton signal at 12.13 ppm in DMSO-d_6 in the ^1H NMR spectra is assigned to the N1−H1···N4 HB (Figure S1, Supporting Information). When the temperature rises above 40 °C, a downfield-shifted peak appears at 13.68 ppm, which might be attributed to the proton in N1−H1···O1 HB of *E*-2-BFP.[25,26] The single absorption peak in solvents and the unique sharp O═C peak at 1704 cm^{-1} in the infrared (IR) (Figure S2, Supporting Information) support the existence of one dominant component of *Z*-2-BFP.[25] In contrast, 4-BFP, missing the intramolecular HB, exhibits the *Z*-form in the ^1H NMR spectra but manifests double O═C peaks at 1740 and 1688 cm^{-1} in the IR, owing to the free rotation about the aryl−alkene bond and the isomerization of the alkene. The seemingly minor structural variation results in different stable forms. In other BFP analogues with similar structures, 4c thermodynamically prefers to the *Z*-isomer as 2-BFP,[25] but 1h is more stable in the *E*-configuration with a seven-membered ring.[26]

The structure of *Z*-2-BFP and the N1−H1···N4 HB are further evidenced by X-ray single-crystal analysis (Figures 2 and S3, Supporting Information). The imidazole and imidazolidinone rings are nearly coplanar (∠N1−C3−C5−N4 = 2.49° and ∠N1−H1−N4−C5 = 0.12°). A six-membered ring is formed with distances of 2.32 Å for N4−H1 and 2.87 Å for N1−N4 and an angle of 120.7° for ∠N1−H1−N4. The N4−H1 distance is longer than the normal proton-acceptor distance by about 2 Å, indicating a weak HB that could be competitively replaced by an intermolecular HB with the solvent in protic solutions. Additionally, the molecules are regularly arranged in the crystal through $\pi-\pi$ interactions with a distance of 3.32 Å between neighboring planes, resulting in the N band of 2-BFP showing a large bathochromic shift from ∼470 nm in solvents to 495 nm in the PMMA film (Figure 3A). On the other hand,

dx.doi.org/10.1021/jz402280w | *J. Phys. Chem. Lett.* 2014, 5, 92−98

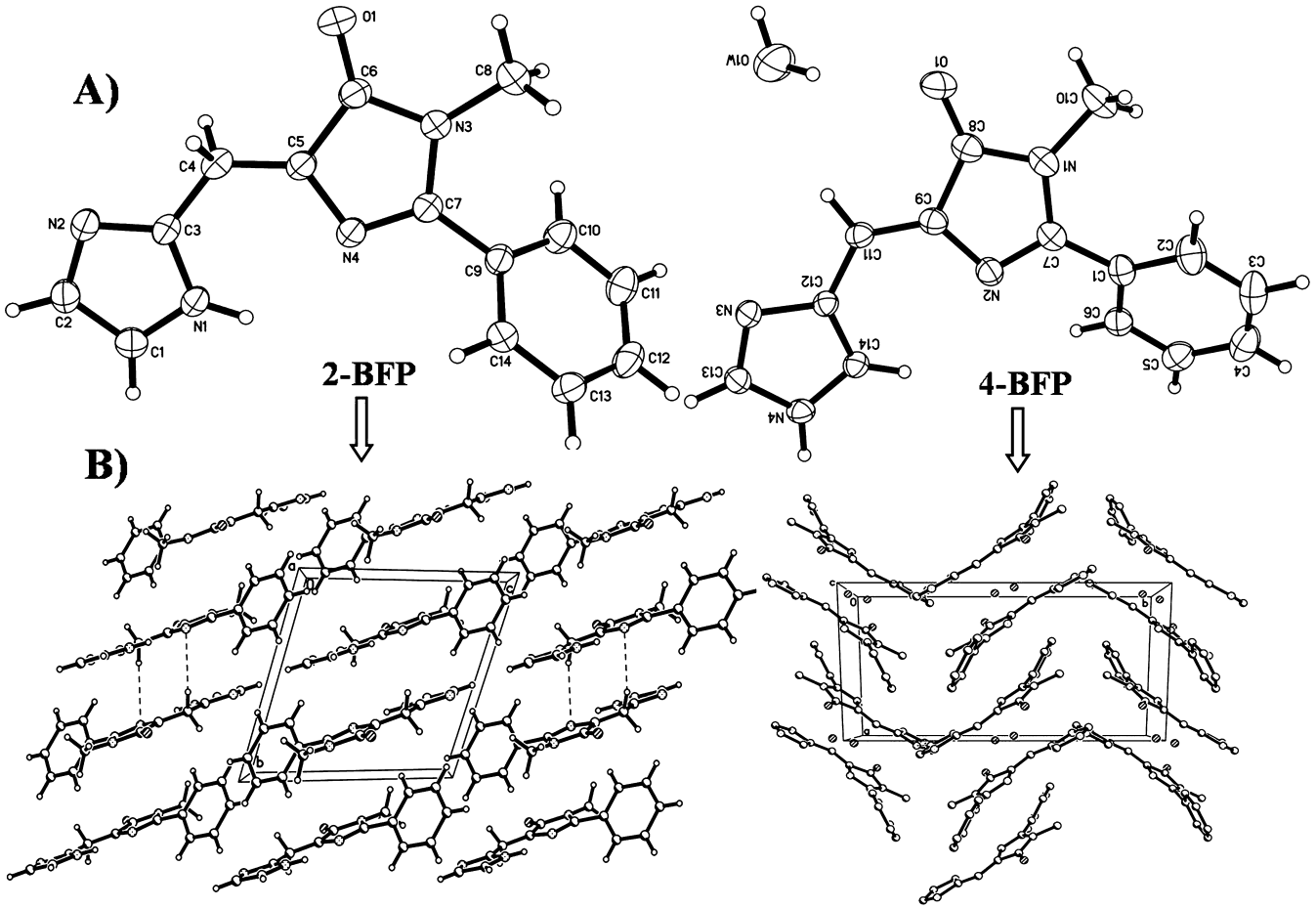

Figure 2. (A) Molecular structures of 2-BFP and 4-BFP. Thermal ellipsoids are drawn at the 50% probability level. (B) The 2D layer structures of 2-BFP and 4-BFP.

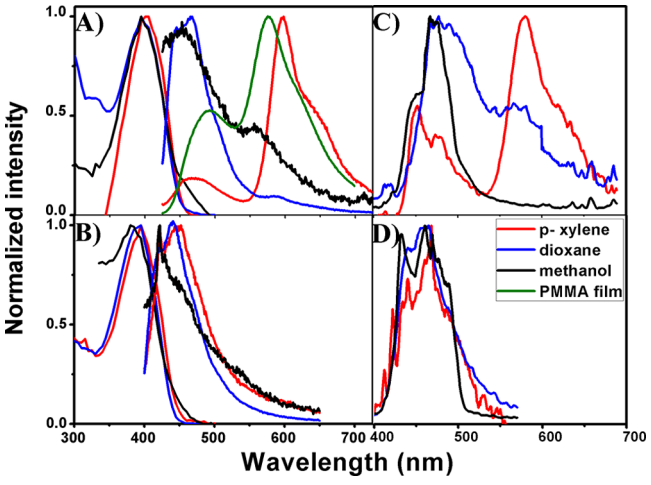

Figure 3. Absorption and fluorescence spectra of (A) 2-BFP and (B) 4-BFP excited at 375 nm in *p*-xylene (red), dioxane (blue), methanol (black), and PMMA film (green) doped with 5 wt % (only with 2-BFP) of each dye at room temperature. Fluorescence spectra of (C) 2-BFP and (D) 4-BFP excited at 375 nm in *p*-xylene, dioxane, and methanol at low temperatures close to the melting point of each solvent in frozen glassy solution.

the T band emissions evidently blue shift (~ 20 nm) in the solid film. These reverse emission shifts of the N and T bands in PMMA indicate that either the $\pi-\pi$ interactions are interrupted in the T state or the T* state is more sensitive to the vibration relaxation involved in aprotic nonpolar solutions. On the contrary, 4-BFP possesses a less planar structure without intermolecular $\pi-\pi$ interactions in the solid crystal.

In aprotic nonpolar solvents, the T band dominates the fluorescence spectra of 2-BFP, while the N band turns out to be a major proportion in a HB accepting solvent such as dioxane, which might be attributed to an equilibrium between the normal *Z*-2-BFP with an intramolecular HB and the "solvated"-2-BFP possessing intermolecular HB with solvents.[29,30] As a result of solvating, both the N and T bands of 2-BFP are greatly blue-shifted. At the same time, the varied ratios of the N/T band emissions lead to color changes from orange in hexane to blue in dioxane.

On the contrary, the quantum yield sharply decreases to 0.01, and no T band appears in the HB donating solvent (MeOH), implying that the intermolecular HB with solvents is the dominant one in MeOH. The resource of the weak band around 556 nm is unclear, possibly arising from certain 2-BFP/methanol complexes. However, as confirmed by the transient absorption (Figure S8D, Supporting Information), it is not from ESIPT. The competition between the intra- and intermolecular HB remarkably decreases the rigidity of 2-BFP, leading to the notable blue shifts of the absorption also (Table 1). At low temperatures, the quantum yields of both 2-BFP and 4-BFP are greatly enhanced ($\varphi_f > 0.2$), owing to the constraint of the motion of the molecules. In addition, the T

dx.doi.org/10.1021/jz402280w | *J. Phys. Chem. Lett.* 2014, 5, 92−98

Table 1. Photophysical Properties of 2-BFP and 4-BFP in Various Solvents[a]

	2-BFP						4-BFP			
	λ_{abs}[b]	λ_{em}[b]	φ_{fN}[c]	φ_{fT}[c]	N band[d,f]	T band[e,f]	λ_{abs}[b]	λ_{em}[b]	φ_f	N band[d]
n-hexane[g]	401	451/594	0.0086	0.0230	2.9(0.65) 11.6(0.35)	3(−0.27) 13.1(−0.57) 937.8(+1.0)	396	472	0.0095	2.0(0.56) 26.2(0.44)
benzene[g]	396	465/595	0.0261	0.0618	2.4(0.56) 12.7(0.44)	2.8(−0.48) 17.5(−0.28) 686.2(+0.40)	393	465	0.0166	2.3(0.60) 17.4(0.40)
p-xylene[g]	407	472/598	0.0205	0.1014	3.7(0.50) 12.9(0.50)	2(−0.44) 18.3(−0.22) 1159.0(+0.37)	396	472	0.0234	2.0(0.56) 26.2(0.44)
dioxane[g]	395	465/584	0.0969	0.0095	2.7(0.63) 18.0(0.36)	2.5(−0.78) 18.0(−0.04) 423.4(+0.08)	393	465	0.0475	2.2(0.56) 13.9(0.44)
MeOH[g]	385	458	0.0108	na	2.4(0.68) 15.8(0.32)		379	464	0.0081	1.3(0.68) 4.8(0.32)
p-xylene[h]		452/580	0.0600	0.1593				468	0.0359	
dioxane[h]		477/566	0.1761	0.1011				465	0.1040	
MeOH[h]		467	0.2473	na				460	0.2342	

[a]Absorption and fluorescence spectra of 2-BFP and 4-BFP are shown in Figure S4 (Supporting Information). [b]Units: nm. [c]The overall quantum yields (φ_f) of the molecule are the sum of φ_{fN} and φ_{fT}. [d]Decay rates are in ps. [e]Rise (−) and decay (+) rates are in ps (at high concentrations, two decay rates of the T band are observed; one originates from the N band overlapping peaks (Figure S7, inset, Supporting Information), and the other one is listed here). [f]The number in parentheses represents the weight of the component. [g]At room temperature. [h]At low temperatures close to the melting points of each solvent in frozen glassy solution.

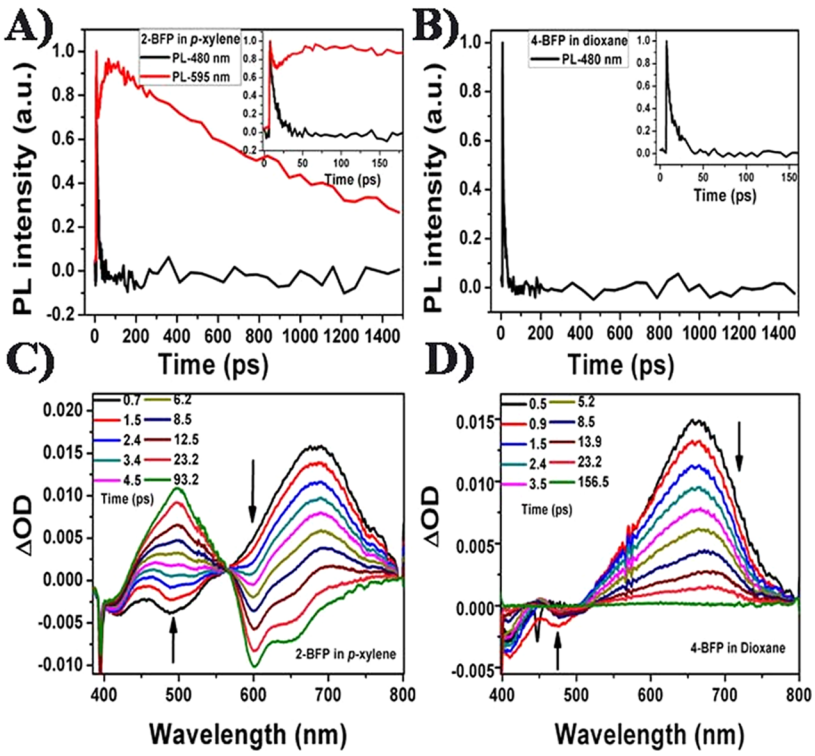

Figure 4. Fluorescence up-conversion transients of 2-BFP in *p*-xylene (A) at 480 and 590 nm and 4-BFP in dioxane (B) at 480 nm. Femtosecond UV/vis transient absorption spectra of 2-BFP in *p*-xylene (C) and 4-BFP in dioxane (D) upon excitation at 400 nm.

bands of 2-BFP are blue-shifted at low temperatures, implying a shrunk π-conjugated system in the tautomer 2-BFP.

Computational calculations with the CamB3LYP/6/311G-(d,p) method show that the electron densities of normal and tautomer 2-BFP species spread on the imidazole and imidazolinone rings in both the HOMOs and LUMOs involved in the S0 → S1 transition (Figure S6, Supporting Information). These large overlaps of the electron might be favored for the emission, contributing to the high quantum yield of 2-BFP that is almost 2 orders of magnitude higher than that of *o*-HBDI. In *o*-HBDI or OHBI (4-(2-hydroxybenzylidene)-1H-imidazol-5(4H)-one), the electron density is mainly located in the phenol fragment in the HOMO but largely transferred to the imidazolone moiety in the LUMO.[31]

dx.doi.org/10.1021/jz402280w | J. Phys. Chem. Lett. 2014, 5, 92−98

Scheme 1. Proposed Schematic ESIPT Reaction of 2-BFP and the Influence of Zn^{2+} Binding on the Proton-Transfer Process

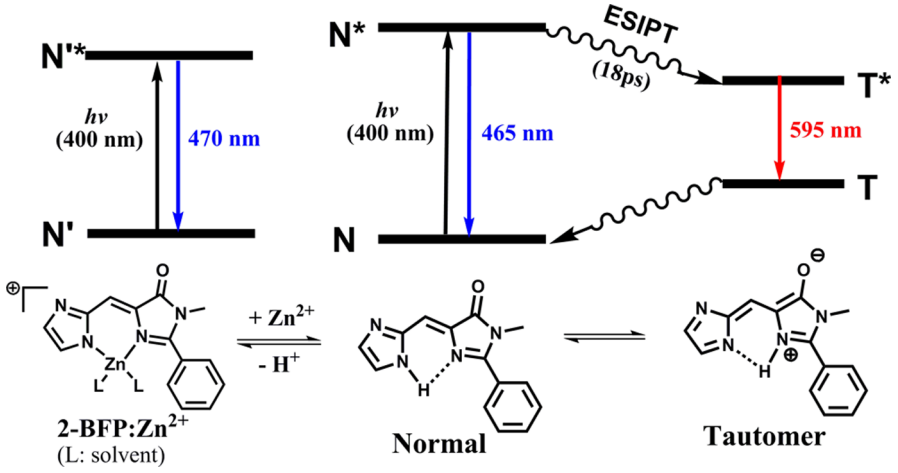

The dynamics of the ESIPT in 2-BFP has been monitored in various solvents. Fluorescence up-conversion (Figures 4 and S7, Supporting Information) shows that the photoluminescent (PL) dynamics of 480 nm has two decaying components, the faster component with a rate of ∼3 ps and the slower one with a rate of ∼18 ps. Correspondingly, PL dynamics of 595 nm has two rising components, about 3 and 18 ps. Both of the rising rates are independent of the solvents. The rise of the T band correlates well with the decay of the N band (within experimental error), supporting the precursor−successor type of relaxation from the same ground-state precursor. Furthermore, the similar dynamics at 635 and 595 nm suggests that the shoulder arises from the same tautomer transition. Thus, these two emissions with a ∼1100 cm^{-1} energy difference might represent different vibrational energy levels caused by the benzene ring attached with imidazolinone. Two or even more decay components have been reported for several ESIPT-resulting emissions.[26,30,32] However, two rise components for ESIPT have not been observed in GFP analogues.

Though the rates at picosecond levels are slow for ESIPT, they are quite fast for normal fluorescence decays. It is noted that the high quantum yield (>0.1) and the short lifetime at picoseconds correlate to a radiative decay rate constant of ∼3 × 10^{10} s^{-1}, which is much faster than the typical rate constants for organic fluorophores. The detailed mechanism leading to these results is unclear, but certainly more complicated processes other than the simple relaxation and proton transfer occurred. For *o*-HBDI, the quantum yield rose to 0.4 in solid films, which accounted for the rigidity enhancement in the film. In 2-BFP, the benzene ring might provide a large barrier in both the N and T forms to preclude free rotation of the aryl−alkene, thus facilitating the fluorescence formation.[33]

Femtosecond transient absorption experiments are applied to track the process of the T* state formation of 2-BFP through the ESIPT reaction (Figures 4 and S8, Supporting Information). The spectra consist of three parts. The spectra from 380 to 450 nm represent the ground-state bleaching (GSB), which resemble its steady-state absorption spectra. The spectra from 450 to 560 nm are the stimulated emission (SE) of the local excited (LE) state, which resemble the PL spectra of the LE state and match the steady-state 472 nm normal emission of 2-BFP in *p*-xylene. Simultaneously, the spectra from 560 to 800 nm are the excited-state absorption (EA) of the LE state. With the time elapsed, the SE and EA of the LE state decay rapidly, with a new SE emerging at 560−800 nm and a new EA emerging at 450−560 nm. The LE state corresponds to the N band, and the new state corresponds to the T band. The converting time constant of ∼18 ps matches with the results from the fluorescence up-conversion studies. On the basis of the steady-state and transient kinetic studies, a schematic ESIPT reaction of 2-BFP is proposed as in Scheme 1. In contrast to 2-BFP, the SE (450−550 nm) and EA (550 - 800 nm) of the LE state of 4-BFP all decay rapidly without the formation of new states (Figure 4D), demonstrating that no ESIPT reaction takes place in 4-BFP.

Both the fluorescence up-conversion technique and femtosecond transient absorption (Figures S7F and S8E, Supporting Information) have shown that the substitution of the proton with a deuteron (H/D) does not alter the proton-transfer rate of 2-BFP, demonstrating that the barrier curbing the proton transfer is not directly related to the motion of the proton itself. Furthermore, even if no ESIPT takes place for 2-BFP in MeOH, the decay rates of the N band are the same as those in other solvents with ESIPT reactions, which further implies that the relaxation of the N* state is not determined by the ESIPT. On the contrary, the relaxation of the excited 2-BFP competitively goes through radiationless and fluorescent emission pathways or triggers proton transfer.

No direct observations can unambiguously assign the exact origination of the decays of the N* state of 2-BFP. The early fast N* decay and T* rise component at several picoseconds might originate from the intramolecular vibrational redistribution,[15] torsional relaxation giving a planar and relaxed configuration,[34] or the electron density redistribution leading to an increased dipole moment stabilized by solvation dynamics in the excited state.[32] In contrast, the ∼18 ps decay might be via a solvent-polarity-independent type of solvation of the molecule, such as a cooling process by collisions with the surrounding solvent[35,36] or by the skeleton rearrangement of the molecule that is insensitive to O−H motion.[23]

In *o*-HBDI, an ultrafast (<25 fs) ESIPT occurs through a barrierless pathway.[15] Differently, in 2-BFP, the picosecond level of ESIPT rates as well as the dual emissions caused by the competitive relaxations through proton-transfer and radiation processes indicate the existence of an energy barrier. The weak photoacidity of the imidazole hydrogen (N−H) relative to the phenolic hydrogen (O−H) is ascribed to such differences. Furthermore, the S0 → S1 $^1\pi\pi^*$ transition is accompanied by a

dx.doi.org/10.1021/jz402280w | J. Phys. Chem. Lett. 2014, 5, 92−98

negative charge transfer in OHBI more markedly than that in 2-BFP, as suggested by their electron density distributions in the HOMO and LUMO (Figure S6, Supporting Information), which would trigger the subsequent transfer of a proton immediately.[31]

The stark different behaviors of 2-BFP and the analogue 1h or 4c demonstrate that the control of ESIPT mediated by N−H···N HB is plausible (Figure S5, Supporting Information). A simple replacement of the pyrrolic ring with the imidazole moiety activates the proton-transfer process. The additional nitrogen atom in the imidazole ring enhances the photoacidity of the N(1)−H via its electron-withdrawing property.[23] Furthermore, theoretical calculations show that high electron density is distributed on the imidazole N(1) atom in the HOMO of 2-BFP (Figure S6, Supporting Information) but not on the pyrrolic N atom in the HOMO of 1h.[26]

It is also noteworthy that the ESIPT and fluorescence of 2-BFP are influenced by the Zn^{2+} binding in organic solvents (Scheme 1 and Figure S5, Supporting Information). In the absence of Zn^{2+}, 2-BFP displays a mixed color from both N and T band emissions. In the presence of Zn^{2+}, the T band emission is prohibited, and the N band emission is enhanced because the Zn^{2+} binding eliminates the intramolecular HB and strengthens the rigidity of the molecule.[37,38] This provides another example and insight for the regulation and application of the molecules with the ESIPT mechanism.

In summary, 2-BFP, a synthetic BFP−chromophore analogue, shows photophysical and photochemical properties different from those of other GFP analogous. It displays both N and T band emissions rising from the same *Z*-isomer, which makes it an excellent template to study the mechanism of dual emissions. The high quantum yield above 0.1 makes it valuable not only for principle investigations but also for practical applications. Two rising lifetime components have been observed for the proton transfer of 2-BFP, and the transfer rates are at picoseconds, which might be more suitable for tracking the detailed process and revealing the mechanism of the proton transfer compared to the ultrafast systems. The relatively weaker photoacidity of N−H compared to O−H determines the different properties of 2-BFP compared to the other GFP analogues. In addition, the diverse behaviors of 2-BFP and 1h (or 4c) demonstrate that the ESIPT mediated through the N−H···N type of HBs can be regulated by tuning the photoacidity of the molecules. Finally, the ESIPT process in 2-BFP can be inhibited in protic solvents (MeOH) or by the formation of metal−chelate complexes (2-BFP/Zn^{2+}). These findings expand our understanding of GFP chromophores and excited-state intramolecular proton-transfer reactions. It provides insights into the further development of novel fluorescent sensors and materials.

■ ASSOCIATED CONTENT

Supporting Information

Synthetic and experimental details, temperature-dependent ^1H NMR spectra of 2-BFP, IR spectra, calculation details, fluorescence up-conversion technique, and femtosecond transient absorption. This material is available free of charge via the Internet at http://pubs.acs.org.

■ AUTHOR INFORMATION

Corresponding Authors

*E-mail: yangwei@ciac.ac.cn (W.Y.).
*E-mail:brgao@jlu.edu.cn (B.-R.G.).
*E-mail: jwxu@ciac.ac.cn (J.X.).

Notes

The authors declare no competing financial interest.

■ ACKNOWLEDGMENTS

We thank the Natural Science Foundation of China (NSFC), Grant Number 30870491 (to W.Y.) for the financial support.

■ REFERENCES

(1) Sullivan, K. F.; Kay, S. A. *Green Fluorescent Proteins*; Academic Press: San Diego, CA, 1999.
(2) Tsien, R. Y. The Green Fluorescent Protein. *Annu. Rev. Biochem.* **1998**, *67*, 509−544.
(3) Zimmer, M. Green Fluorescent Protein (GFP): Applications, Structure, and Related Photophysical Behavior. *Chem. Rev.* **2002**, *102*, 759−782.
(4) Chudakov, D. M.; Matz, M. V.; Lukyanov, S.; Lukyanov, K. A. Fluorescent Proteins and Their Applications in Imaging Living Cells and Tissues. *Physiol. Rev.* **2010**, *90*, 1103−1163.
(5) Shcherbakova, D. M.; Subach, O. M.; Verkhusha, V. V. Red Fluorescent Proteins: Advanced Imaging Applications and Future Design. *Angew. Chem., Int. Ed.* **2012**, *51*, 10724−10738.
(6) Heim, R.; Prasher, D. C.; Tsien, R. Y. Wavelength Mutations and Posttranslational Autoxidation of Green Fluorescent Protein. *Proc. Natl. Acad. Sci. U.S.A.* **1994**, *91*, 12501−12504.
(7) Shaner, N. C.; Patterson, G. H.; Davidson, M. W. Advances in Fluorescent Protein Technology. *J. Cell Sci.* **2007**, *120*, 4247−4260.
(8) Baranov, M. S.; Lukyanov, K. A.; Yampolsky, I. V. Synthesis of the Chromophores of Fluorescent Proteins and Their Analogs. *Russ. J. Bioorg. Chem.* **2013**, *39*, 223−244.
(9) Tolbert, L. M.; Baldridge, A.; Kowalik, J.; Solntsev, K. M. Collapse and Recovery of Green Fluorescent Protein Chromophore Emission through Topological Effects. *Acc. Chem. Res.* **2012**, *45*, 171−181.
(10) He, X.; Bell, A. F.; Tonge, P. J. Synthesis and Spectroscopic Studies of Model Red Fluorescent Protein Chromophores. *Org. Lett.* **2002**, *4*, 1523−1526.
(11) Stoner-Ma, D.; Jaye, A. A.; Ronayne, K. L.; Nappa, J.; Meech, S. R.; Tonge, P. J. An Alternate Proton Acceptor for Excited-State Proton Transfer in Green Fluorescent Protein: Rewiring GFP. *J. Am. Chem. Soc.* **2008**, *130*, 1227−1235.
(12) Dong, J.; Solntsev, K. M.; Poizat, O.; Tolbert, L. M. The Meta-Green Fluorescent Protein Chromophore. *J. Am. Chem. Soc.* **2007**, *129*, 10084−10085.
(13) Solntsev, K. M.; Poizat, O.; Dong, J.; Rehault, J.; Lou, Y. B.; Burda, C.; Tolbert, L. M. Meta and Para Effects in the Ultrafast Excited-State Dynamics of the Green Fluorescent Protein Chromophores. *J. Phys. Chem. B* **2008**, *112*, 2700−2711.
(14) Chen, K. Y.; Cheng, Y. M.; Lai, C. H.; Hsu, C. C.; Ho, M. L.; Lee, G. H.; Chou, P. T. Ortho Green Fluorescence Protein Synthetic Chromophore; Excited-State Intramolecular Proton Transfer via a Seven-Membered-Ring Hydrogen-Bonding System. *J. Am. Chem. Soc.* **2007**, *129*, 4534−4535.
(15) Hsieh, C. C.; Chou, P. T.; Shih, C. W.; Chuang, W. T.; Chung, M. W.; Lee, J.; Joo, T. Comprehensive Studies on an Overall Proton Transfer Cycle of the *ortho*-Green Fluorescent Protein Chromophore. *J. Am. Chem. Soc.* **2011**, *133*, 2932−2943.
(16) Baranov, M. S.; Lukyanov, K. A.; Borissova, A. O.; Shamir, J.; Kosenkov, D.; Slipchenko, L. V.; Tolbert, L. M.; Yampolsky, I. V.; Solntsev, K. M. Conformationally Locked Chromophores as Models of Excited-State Proton Transfer in Fluorescent Proteins. *J. Am. Chem. Soc.* **2012**, *134*, 6025−6032.
(17) Chou, P. T. The Host/Guest Type of Excited-State Proton Transfer; A General Review. *J. Chin. Chem. Soc.* **2001**, *48*, 651−682.
(18) Uzhinov, B. M.; Khimich, M. N. Conformational Effects in Excited State Intramolecular Proton Transfer of Organic Compounds. *Russ. Chem. Rev.* **2011**, *80*, 553−577.

(19) Kwon, J. E.; Park, S. Y. Advanced Organic Optoelectronic Materials: Harnessing Excited-State Intramolecular Proton Transfer (ESIPT) Process. *Adv. Mater.* **2011**, *23*, 3615−3642.
(20) Kwon, J. E.; Park, S.; Park, S. Y. Realizing Molecular Pixel System for Full-Color Fluorescence Reproduction: RGB-Emitting Molecular Mixture Free from Energy Transfer Crosstalk. *J. Am. Chem. Soc.* **2013**, *135*, 11239−11246.
(21) Waluk, J. Hydrogen-Bonding-Induced Phenomena in Bifunctional Heteroazaaromatics. *Acc. Chem. Res.* **2003**, *36*, 832−838.
(22) Piwoński, H.; Sokołowski, A.; Kijak, M.; Nonell, S.; Waluk, J. Arresting Tautomerization in a Single Molecule by the Surrounding Polymer: 2,7,12,17-Tetraphenyl Porphycene. *J. Phys. Chem. Lett.* **2013**, *4*, 3967−3971.
(23) Yu, W. S.; Cheng, C. C.; Cheng, Y. M.; Wu, P. C.; Song, Y. H.; Chi, Y.; Chou, P. T. Excited-State Intramolecular Proton Transfer in Five-Membered Hydrogen-Bonding Systems: 2-Pyridyl Pyrazoles. *J. Am. Chem. Soc.* **2003**, *125*, 10800−10801.
(24) Kijak, M.; Nosenko, Y.; Singh, A.; Thummel, R. P.; Waluk, J. Mode-Selective Excited-State Proton Transfer in 2-(2′-Pyridyl)pyrrole Isolated in a Supersonic Jet. *J. Am. Chem. Soc.* **2007**, *129*, 2738−2739.
(25) Wu, L. X.; Burgess, K. Syntheses of Highly Fluorescent GFP-Chromophore Analogues. *J. Am. Chem. Soc.* **2008**, *130*, 4089−4096.
(26) Chuang, W. T.; Hsieh, C. C.; Lai, C. H.; Lai, C. H.; Shih, C. W.; Chen, K. Y.; Hung, W. Y.; Hsu, Y. H.; Chou, P. T. Excited-State Intramolecular Proton Transfer Molecules Bearing *o*-Hydroxy Analogues of Green Fluorescent Protein Chromophore. *J. Org. Chem.* **2011**, *76*, 8189−8202.
(27) Fang, X.; Li, H.; Zhao, G.; Fang, X.; Xu, J.; Yang, W. Blue Fluorescent Protein Analogues as Chemosensors for Zn^{2+}. *Biosens. Bioelectron.* **2013**, *42*, 308−313.
(28) Chou, P. T.; Pu, S. C.; Cheng, Y. M.; Yu, W. S.; Yu, Y. C.; Hung, F. T.; Hu, W. P. Femtosecond Dynamics on Excited-State Proton Charge-Transfer Reaction in 4′-*N*,*N*-Diethylamino-3-hydroxyflavone. The Role of Dipolar Vectors in Constructing a Rational Mechanism. *J. Phys. Chem. A* **2005**, *109*, 3777−3787.
(29) Kasha, M. Proton-Transfer Spectroscopy — Perturbation of the Tautomerization Potential. *J. Chem. Soc., Faraday Trans. 2* **1986**, *82*, 2379−2392.
(30) Abou-Zied, O. K.; Jimenez, R.; Thompson, E. H. Z.; Millar, D. P.; Romesberg, F. E. Solvent-Dependent Photoinduced Tautomerization of 2-(2′-Hydroxyphenyl)benzoxazole. *J. Phys. Chem. A* **2002**, *106*, 3665−3672.
(31) Cui, G. L.; Lan, Z. G.; Thiel, W. Intramolecular Hydrogen Bonding Plays a Crucial Role in the Photophysics and Photochemistry of the GFP Chromophore. *J. Am. Chem. Soc.* **2012**, *134*, 1662−1672.
(32) Conyard, J.; Kondo, M.; Heisler, I. A.; Jones, G.; Baldridge, A.; Tolbert, L. M.; Solntsev, K. M.; Meech, S. R. Chemically Modulating the Photophysics of the GFP Chromophore. *J. Phys. Chem. B* **2011**, *115*, 1571−1576.
(33) Yang, J. S.; Chiou, S. Y.; Liau, K. L. Fluorescence Enhancement of *trans*-4-Aminostilbene by *N*-Phenyl Substitutions: The "Amino Conjugation Effect". *J. Am. Chem. Soc.* **2002**, *124*, 2518−2527.
(34) Douhal, A.; Sanz, M.; Carranza, M. A.; Organero, J. A.; Santos, L. Femtosecond Observation of Intramolecular Charge- and Proton-Transfer Reactions in a Hydroxyflavone Derivative. *Chem. Phys. Lett.* **2004**, *394*, 54−60.
(35) Chou, P. T.; Chen, Y. C.; Yu, W. S.; Chou, Y. H.; Wei, C. Y.; Cheng, Y. M. Excited-State Intramolecular Proton Transfer in 10-Hydroxybenzo[h]quinoline. *J. Phys. Chem. A* **2001**, *105*, 1731−1740.
(36) Zhong, D. P.; Douhal, A.; Zewail, A. H. Femtosecond Studies of Protein−Ligand Hydrophobic Binding and Dynamics: Human Serum Albumin. *Proc. Natl. Acad. Sci. U.S.A.* **2000**, *97*, 14056−14061.
(37) Henary, M. M.; Fahrni, C. J. Excited State Intramolecular Proton Transfer and Metal Ion Complexation of 2-(2′-Hydroxyphenyl)benzazoles in Aqueous Solution. *J. Phys. Chem. A* **2002**, *106*, 5210−5220.
(38) Udhayakumari, D.; Saravanamoorthy, S.; Ashok, M.; Velmathi, S. Simple Imine Linked Colorimetric and Fluorescent Receptor for Sensing Zn^{2+} Ions in Aqueous Medium Based on Inhibition of ESIPT Mechanism. *Tetrahedron Lett.* **2011**, *52*, 4631−4635.